Deep-Sea Research, Vol. 31, No. 12, pp. 1395 to 1414, 1984.
Printed in Great Britain.

0198–0149/84 $3.00 + 0.00

Oscillatory drift of deep cold eddies

DORON NOF*

(*Received* 8 *August* 1983; *in revised form* 23 *February* 1984; *accepted* 1 *June* 1984)

Abstract—This paper supplements an earlier one on the dynamics of cold isolated eddies situated on a sloping oceanic floor (NOF, 1983a, *Deep-Sea Research*, **29**, 171–182). The lens-like eddies under investigation correspond to cold patches bounded by an interface that intersects the sloping floor along a closed curve. A wide range of possible time-dependent migration patterns is explored analytically. Nonlinear solutions are constructed by separating the equations governing the migration from those governing the eddy's interior.

It is shown that, in addition to the known steady migration at 90° to the right of the downhill direction discussed previously, oscillatory migration is also possible. This time-dependent migration corresponds to a nonlinear eddy that drifts along a cycloid. The asymmetrical oscillations are of the inertial period. They are superimposed on a main migration path which, as in the steady migration case, is directed along a straight line whose orientation is at 90° to the right of the downhill slope. To an observer riding with the eddy, the circulation within the eddy appears to be steady whereas the migration is time dependent. As in the steady translation case, the drift is entirely independent of the eddy's size, intensity, and depth. It depends only on the density difference between the eddy and the environment, the gravitational acceleration, the bottom slope, and the Coriolis parameter.

Application of this theory to various eddies situated on the ocean floor is discussed.

INTRODUCTION

RECENTLY, attention has been drawn to isolated pools of anomalous cold water on the ocean bottom. HOUGHTON *et al.* (1982) and OU and HOUGHTON (1982) conducted a comprehensive study of a cold-pool in the Mid-Atlantic Bight, ARMI and D'ASARO (1980) identified isolated cold patches on the abyssal plane, and EBBESMEYER (personal communication) observed (during POLYMODE) a cold isolated 'blob' on the ocean floor near 70°W and 25°N. The length, depth, and temperature anomalies of these blobs vary considerably from one kind of patch to another. Overall the range of the length, speed, depth, and temperature scales is 10 to 100 km, 1 to 10 cm s^{-1}, 20 to 200 m, and 0.05 to 4°C, respectively.

On the basis of theoretical considerations, NOF (1983a) recently suggested that such blobs will migrate whenever they are situated over a sloping bottom. The suggested migration results from the gravitational force which tends to pull the blobs toward the deepest portions of the ocean and the Coriolis force which tends to deflect the blob toward the right. The balance of these two forces takes place in such a way that a steady translation at 90° to the right of the downhill direction is established. The migration, occurring along lines of constant depth, can be relatively fast. It is given by $g(\Delta\rho/\rho)(S/f)$ (where ρ and $\Delta\rho$ are the density and the density difference between the blob and its environment, g is the gravitational acceleration, S the slope of the bottom, and f is the Coriolis parameter); therefore the migration can reach values as high as 5 to 20 cm s^{-1}.

* Department of Oceanography, The Florida State University, Tallahassee, FL 32306, U.S.A.

The observations of HOUGHTON *et al.* (1982) and OU and HOUGHTON (1982) show that the cold pools do indeed migrate in a manner similar to that suggested by the model. The migration is in the same direction as predicted, and the observed drift ($\sim$3 cm s^{-1}) is close to the predicted speed* ($\sim$5 cm s^{-1}, corresponding to $\Delta\rho/\rho = 5 \times 10^{-4}$, $S = 10^{-3}$, and $f = 10^{-4}$ s^{-1}). This general agreement is suggestive but the original model left a number of important questions unanswered. Among these questions are the possibility that the steady translation is not the sole solution to the problem and the possibility that a shallow upper layer may alter the migration by introducing form drag and 'lift'. In this paper we shall focus on the former issue, namely, the possibility that there are other solutions.

The possibility that an additional solution (corresponding to oscillatory migration) might exist was recently suggested by KILLWORTH (1983). We shall see that an oscillatory drift is indeed possible and that this kind of drift is different from the steady migration case. The distinctive feature of oscillatory migration is that the eddy's center describes a cycloid whose main direction is similar to that of the steady migration, i.e., at 90° to the right of the downhill slope. The oscillations, which are superimposed on this main path, correspond to a total eddy movement up and down the sloping bottom.

The approach that will be used in this paper is to transform the equations of motion to a coordinate system moving with the eddy and then to solve the problem by separating the time-dependent translation from the circulation within the eddy. This partition enables one to construct two separate sets of governing equations. One describes the eddy's translation and the other governs the eddy's circulation.

After presenting the general solution, the results are analyzed in detail and a description of the particles' expected path is given. With the aid of this description it is shown that, due to the orbital motion within the eddy and the general oscillatory translation, the trajectories are complicated and, in some cases, display unusual patterns. The paper is concluded with a discussion of our model's applicability to various eddies on the ocean floor. It is suggested that for moderate eddies ($l \sim 50$ km) at high and mid-latitudes ($f \sim 10^{-4}$ s^{-1}), the ratio between the oscillation amplitude and the eddy radius is small, causing the oscillatory translation path to be fairly close to the steady translation path. Small eddies ($l \sim 10$ km) at low latitudes, on the other hand, may have oscillatory amplitudes of the same order as their radii so that their oscillatory translation paths can be quite different from the steady translation path. The importance of the oscillatory migration results from the fact that, whether the oscillations associated with the general path are small or large (compared to the eddy's size), the oscillatory speeds of deep-ocean eddies (5 to 10 cm s^{-1}) are of the same order as the swirl speed [0(1 to 10) cm s^{-1}]. Consequently, a fixed instrument measuring the speed of the fluid in an eddy that is passing by would sense the oscillations even when the eddy's general path is very close to the steady drift path.

FORMULATION

Consider the two-layer model shown in Fig. 1; the eddy's density and depth are $(\rho + \Delta\rho)$ and h, respectively, and the infinitely deep upper fluid is taken to be at rest.

For convenience, we may assume that the eddy has been suddenly placed on the sloping bottom by, say, a collapse of a cylinder containing fluid whose density is $(\rho + \Delta\rho)$. Instead of

* While encouraging, the comparison is not conclusive for two reasons. First, it has been suggested that the migration can also be a result of advection by a mean flow (OU and HOUGHTON, 1982). Secondly, it is not entirely clear that the fluid above the observed pool can be taken to be infinitely deep as assumed in the original model.

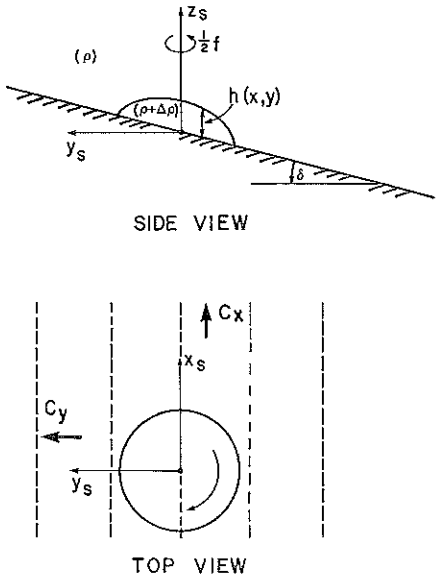

Fig. 1. Schematic diagram of the model under study. The isolated eddy is situated on a sloping bottom ($S = \tan\delta$) and is embedded in an infinitely deep fluid. Dashed lines denote the isobaths. The eddy is translating at an unsteady speed $(C_x^2 + C_y^2)^{1/2}$; its center is initially located at $x_s = y_s = 0$. The subscript 's' indicates association with a stationary frame of reference.

looking for steady translatory states (considered previously), we shall seek time-dependent solutions. We begin by considering the usual shallow water equations for the movement of the eddy:

$$\frac{\partial \mathbf{u}_s}{\partial t_s} + \mathbf{u}_s \cdot \nabla_H \mathbf{u}_s + f\,\mathbf{k}\times\mathbf{u}_s + \frac{1}{\rho}\nabla_H p = 0, \tag{1}$$

$$\frac{\partial h}{\partial t_s} + \nabla_H \cdot (h\mathbf{u}_s) = 0, \tag{2}$$

where $\mathbf{u}_s$ is the horizontal (two-dimensional) velocity vector, ∇_H the horizontal del-operator, p the deviation of the hydrostatic pressure from its motionless value, and h the eddy depth; the subscript 's' denotes that the variable in question is associated with a stationary frame of reference located at the center of the eddy in its initial position. The axes of this coordinate system (x_s and y_s) are directed at 90° and 180° to the left of the downhill direction and the system rotates uniformly about the vertical axis.

The set (1) and (2) is subject to the boundary conditions:

$$C_x = C_y = 0, \qquad t_s = 0, \tag{3}$$

$$h_s = 0, \qquad \gamma_s(x_s, y_s, t_s) = 0, \tag{4a}$$

$$\mathbf{dr} \times (u_s\mathbf{i} + v_s\mathbf{j}) = 0, \qquad h_s = 0, \tag{4b}$$

where $\mathbf{r}$ is the position vector $(x_s\mathbf{i} + y_s\mathbf{j})$. Condition (3) corresponds to the fact that when the

eddy is initially formed, it has no translation in either the x_s or the y_s direction. Condition (4a) states that the eddy's depth vanishes along an unknown curve $\gamma_s = 0$ and (4b) reflects the condition that this curve must be a streamline.

To examine the movements of the eddy, the governing equations are transformed to a coordinate system moving with the eddy's center, i.e., the point where the swirl velocity vanishes:

$$\left.\begin{aligned} x &= x_s - \int_0^{t_s} C_x \, dt_s, \\ y &= y_s - \int_0^{t_s} C_y \, dt_s, \\ u &= u_s - C_x, \qquad v = v_s - C_y, \\ h &= h_s, \qquad t = t_s, \qquad p = p_s, \end{aligned}\right\} \tag{5a}$$

where C_x and C_y are the translation speeds in the x_s and y_s directions, which are taken to be functions only of time [i.e., $C_x = C_x(t_s)$, $C_y = C_y(t_s)$], and the variables without subscripts correspond to the moving coordinate system. Since the time t_s is now a function of x, y, and t [i.e., $\partial/\partial t_s = (\partial/\partial x)(\partial x/\partial t_s) + (\partial/\partial y)(\partial y/\partial t_s) + (\partial/\partial t)(\partial t/\partial t_s)$], the time and space derivatives corresponding to (5a) are

$$\left.\begin{aligned} \frac{\partial}{\partial t_s} &= -C_x \frac{\partial}{\partial x} - C_y \frac{\partial}{\partial y} + \frac{\partial}{\partial t}, \\ \frac{\partial}{\partial x_s} &= \frac{\partial}{\partial x}, \qquad \frac{\partial}{\partial y_s} = \frac{\partial}{\partial y}. \end{aligned}\right\} \tag{5b}$$

In terms of the new variables (defined by 5a) and the corresponding derivatives (given by 5b), the governing equations are

$$\frac{\partial u}{\partial t} + \frac{\partial C_x}{\partial t} + u\frac{\partial u}{\partial x} + v\frac{\partial u}{\partial y} - f(v + C_y) = -\frac{1}{\rho}\frac{\partial p}{\partial x}, \tag{6}$$

$$\frac{\partial v}{\partial t} + \frac{\partial C_y}{\partial t} + u\frac{\partial v}{\partial x} + v\frac{\partial v}{\partial y} + f(u + C_x) = -\frac{1}{\rho}\frac{\partial p}{\partial y}, \tag{7}$$

$$\frac{\partial h}{\partial t} + \frac{\partial}{\partial x}(hu) + \frac{\partial}{\partial y}(hv) = 0, \tag{8}$$

where p, the deviation of the hydrostatic pressure from the pressure associated with a state of rest (i.e., a no blob state), is

$$p = g\,\Delta\rho(h + Sy - z), \tag{9}$$

where S is the bottom slope.

It is further assumed (and later verified) that the eddy's velocities u and v and the eddy's depth h are independent of t so that the eddy's shape remains unaltered as it is translating. Under such conditions only the translation speeds C_x and C_y are functions of time and (6) to (9) take the form

$$\frac{\partial C_x}{\partial t} + u\frac{\partial u}{\partial x} + v\frac{\partial u}{\partial y} - f(v + C_y) = -g'\frac{\partial h}{\partial x}, \tag{10}$$

$$\frac{\partial C_y}{\partial t} + u\frac{\partial v}{\partial x} + v\frac{\partial v}{\partial y} + f(u + C_x) = -g'\frac{\partial h}{\partial y} - g'S, \tag{11}$$

$$\frac{\partial}{\partial x}(hu) + \frac{\partial}{\partial y}(hv) = 0, \tag{12}$$

where $g' = g(\Delta\rho/\rho)$.

The boundary conditions in our new moving coordinate system remain similar to those of the stationary coordinate system (3 and 4) and can be written in the form

$$C_x = C_y = 0, \qquad t = 0, \tag{13}$$

$$h(x, y) = 0, \qquad \gamma(x, y) = 0, \tag{14a}$$

$$(u\mathbf{i} + v\mathbf{j}) \cdot \nabla h = 0, \qquad h(x, y) = 0, \tag{14b}$$

where, for convenience, we have expressed the requirement that the eddy's edge be a streamline in terms of the eddy's depth (h).

SOLUTION

To derive the general solution, it is recalled that we have assumed that u, v, and h are functions of x and y alone [i.e., $u = u(x, y)$; $v = v(x, y)$; $h = h(x, y)$] and that C_x and C_y are functions only of time [i.e., $C_x = C_x(t)$; $C_y = C_y(t)$]. Hence, separation of the terms that contain t from those that contain x and y alone shows that (10) to (12) can be partitioned to the two independent sets:

$$\left.\begin{aligned} \frac{\partial C_x}{\partial t} - fC_y &= 0, \\ \frac{\partial C_y}{\partial t} + fC_x &= -g'S, \end{aligned}\right\} \tag{15}$$

$$\left.\begin{aligned} u\frac{\partial u}{\partial x} + v\frac{\partial u}{\partial y} - fv &= -g'\frac{\partial h}{\partial x}, \\ u\frac{\partial v}{\partial x} + v\frac{\partial v}{\partial y} + fu &= -g'\frac{\partial h}{\partial y}, \\ \frac{\partial}{\partial x}(hu) + \frac{\partial}{\partial y}(hv) &= 0. \end{aligned}\right\} \tag{16}$$

The solution of (15) that satisfies (13) is

$$C_x = -\frac{g'S}{f}(1-\cos ft),$$

$$C_y = -\frac{g'S}{f}\sin ft, \tag{17}$$

and the solution of (16) that satisfies (14) consists of *any* radially symmetric structure. The latter can easily be demonstrated by writing (16) in polar coordinates (r, θ) and setting $\partial/\partial\theta = 0$ and $v_r = 0$. This gives the single equation

$$\frac{v_\theta^2}{r} + fv_\theta = g'\frac{\partial h}{\partial r} \tag{18}$$

that is satisfied by any radially symmetric speed $[v_\theta(r)]$ as stated above. Namely, any interior structure whose circulation is purely tangential satisfies the governing equation and the boundary conditions. One may consider, for instance, eddies with uniform potential vorticity (CSANADY, 1979; FLIERL, 1979) or eddies with a linear (or parabolic) orbital velocity (NOF, 1981, 1982; KILLWORTH, 1983). We shall consider eddies with a linear velocity structure before examining eddies with a parabolic orbital velocity. It should be kept in mind, however, that this choice is strictly a matter of convenience; our general solution is not restricted to any particular internal structure.

A radially symmetric eddy with a linear orbital velocity obeys

$$u = R_0 fy, \qquad v = -R_0 fx,$$

and

$$h = \hat{h} - R_0 f^2(1 - R_0)(x^2 + y^2)/2g', \tag{19}$$

where $\hat{h}$ is the maximum eddy depth $[\hat{h} = h(0, 0)]$ and R_0, the Rossby number, measures the strength of the vortex. With the aid of (19) and (17), the total solution, in the fixed coordinate system, can be written in the form

$$u_s = R_0 f\left[y_s + \frac{g'S}{f^2}(1-\cos ft_s)\right] - \frac{g'S}{f}(1-\cos ft_s), \tag{20a}$$

$$v_s = R_0 f\left[x_s + \frac{g'S}{f}\left(t_s - \frac{1}{f}\sin ft_s\right)\right] - \frac{g'S}{f}\sin ft_s, \tag{20b}$$

$$h_s = \hat{h} - R_0 f^2(1-R_0)\left\{\left[x_s + \frac{g'S}{f}\left(t_s - \frac{1}{f}\sin ft_s\right)\right]^2 + \left[y_s + \frac{g'S}{f^2}(1-\cos ft_s)\right]^2\right\}\Big/2g'. \tag{20c}$$

Equations (20a) to (20c) satisfy the governing equations and boundary conditions with which we started (i.e., 1 to 4), and hence represent a valid solution to the problem. This demonstrates that our original assumptions regarding the independence of u, v, and h on t and the independence of C_x and C_y on x and y are satisfied.

To obtain the equations describing the trajectories, the speeds u_s and v_s in (20a–c) are replaced by dx_s/dt_s and dy_s/dt_s, and the resulting equations are solved by eliminating either x_s or y_s, using elementary methods. The result is

$$X_s(t_s) = r_i \cos[-R_0 f t_s + \theta_i] - \frac{g'S}{f^2}(f t_s - \sin f t_s), \tag{21a}$$

$$Y_s(t_s) = r_i \sin[-R_0 f t_s + \theta_i] - \frac{g'S}{f^2}(1 - \cos f t_s), \tag{21b}$$

where $X_s(t)$ and $Y_s(t)$ correspond to the particle's position in the fixed coordinate system and, for convenience, the initial ($t_s = 0$) particle position is expressed in polar coordinates (r_i, θ_i). These equations are of interest because they correspond to the expected paths of neutrally buoyant floats (such as the SOFAR floats) which are frequently used to track isolated eddies (McDowell and Rossby, 1978). Their properties will be discussed in the next section.

The solution for an eddy with a linear orbital speed (20a–c) and (21a, b) as well as that for eddies with a parabolic orbital speed (A1 to A5; see Appendix) have the following properties: (a) The eddy migrates in an oscillatory manner along a cycloid (Fig. 2). Both the wavelength and the amplitude are of $0(g'S/f^2)$; the period is inertial $[0(f^{-1})]$. (b) The circulation within the eddy is time independent so that the eddy does not change its shape and structure with time (see 19).

ANALYSIS

General properties

As already mentioned, the solution describes an eddy whose center translates along a cycloid. It is easy to show that, as in Nof (1983a), the eddy is migrating as if it were a solid body with a density $(\rho + \Delta\rho)$. To illustrate this point, (10) and (11) are integrated over the whole eddy; after some manipulations (similar to those described in Nof, 1983a) one finds

$$\int\int_{\tilde{r}} \frac{\partial C_x}{\partial t} h \, dx \, dy - \int\int_{\tilde{r}} f h C_y \, dx \, dy = 0, \tag{22}$$

$$\int\int_{\tilde{r}} \frac{\partial C_y}{\partial t} h \, dx \, dy + \int\int_{\tilde{r}} f C_x h \, dx \, dy = -\int\int_{\tilde{r}} g' S h \, dx \, dy, \tag{23}$$

where $\tilde{r}$ denotes the area of the eddy (in the moving coordinate system). These equations describe the total balance of forces acting on the eddy in both the x and y directions. Since C_x and C_y are independent of x and y, (22) and (23) are essentially identical to (15) and (16) multiplied by the volume of the eddy. These equations are equivalent to the elementary equations governing the path of a solid ball rolling on an inclined plane showing that, as mentioned above, the eddy behaves as if it were a solid body.

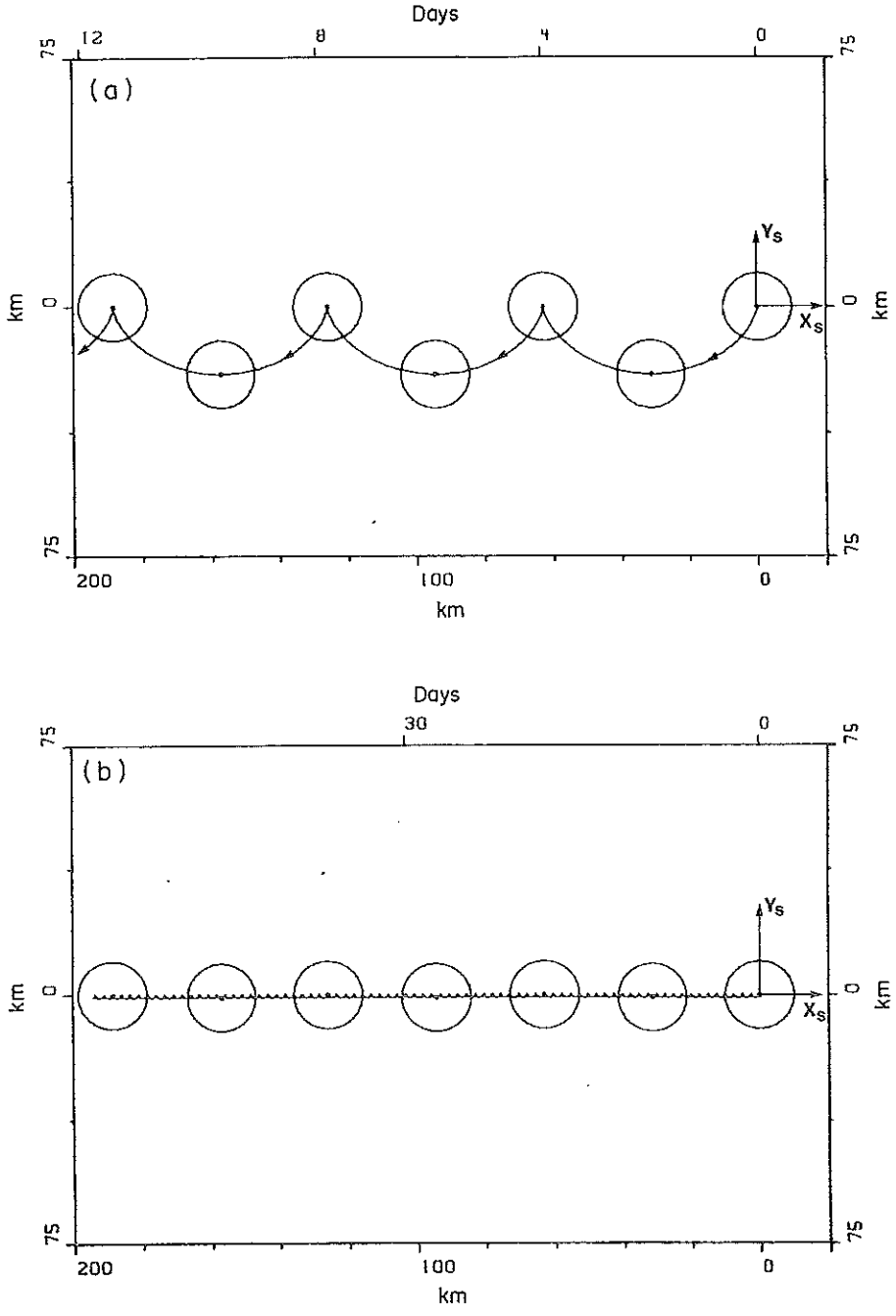

Fig. 2. (a) A typical oscillatory migration pattern of a deep isolated eddy in low latitudes ($g' = 2 \times 10^{-4}$ m s^{-2}, $S = 0.02$, $f = 2 \times 10^{-5}$ s^{-1}, $r_0 = 10$ km). Note that the eddy is drifting along a cycloid. (b) The same as (a) but for an eddy in mid-latitudes ($g' = 2 \times 10^{-4}$ m s^{-2}, $S = 0.02$, $f = 10^{-4}$ s^{-1}, $r_0 = 10$ km). Note that the effect on the migration path is more pronounced in low latitudes (a) than in mid-latitudes.

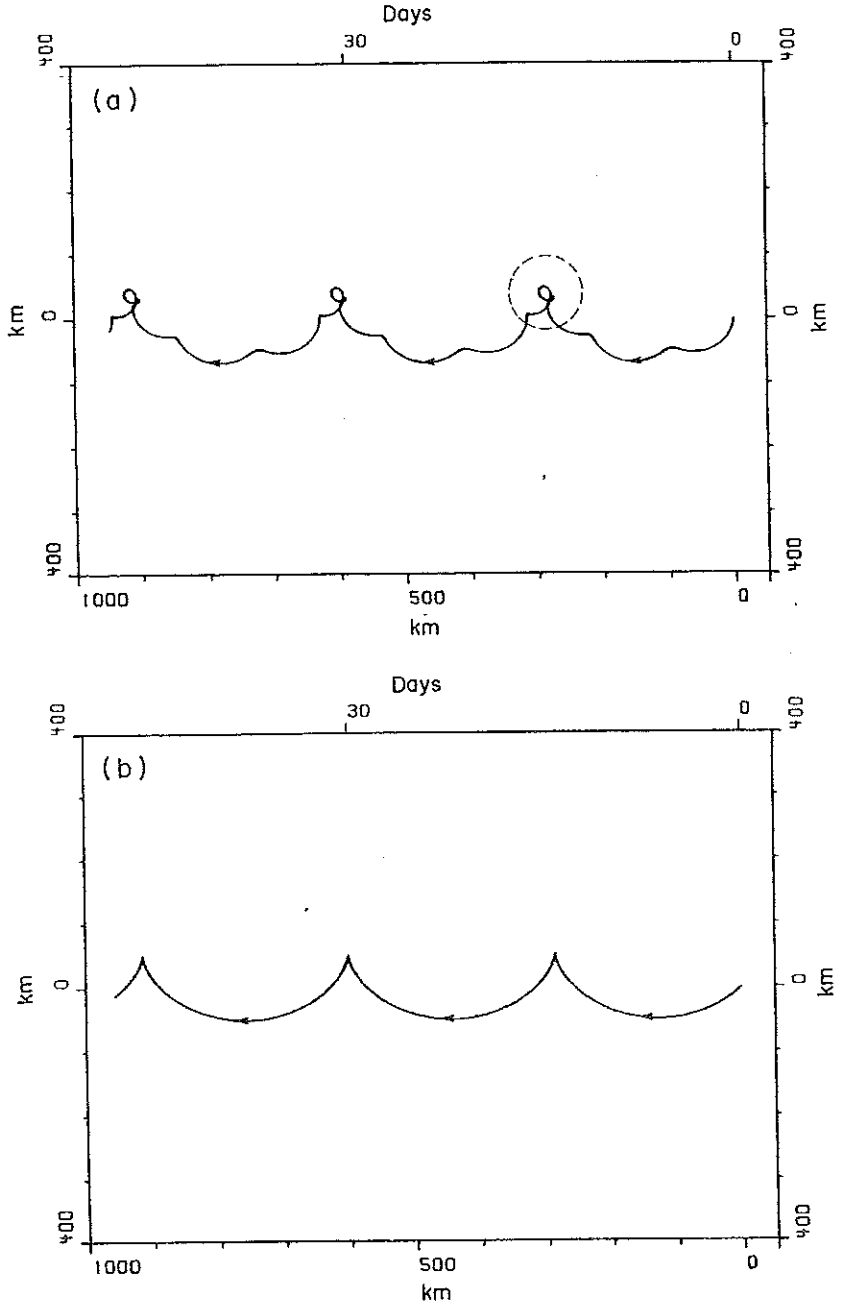

Fig. 3. (a) The general oscillatory trajectory of a particle located at the edge of a typical deep-ocean eddy with a linear orbital velocity in low altitudes ($g' = 2 \times 10^{-4}$ m s^{-2}, $S = 0.02$, $f = 2 \times 10^{-5}$ s^{-1}, $r_0 = 50$ km, $R_0 = 0.2$). The details of the trajectory in the area bounded by the dashed circle are shown in Fig. 4. Note that the trajectory is periodic because, for this particular case, the ratio between frequency of the orbital motion and the oscillatory frequency is a rational number. This is not the most general case because the ratio of the frequencies can take any value.
(b) The same as (a) but for a steady drift ($C_x = -g'S/f$, $C_y = 0$).

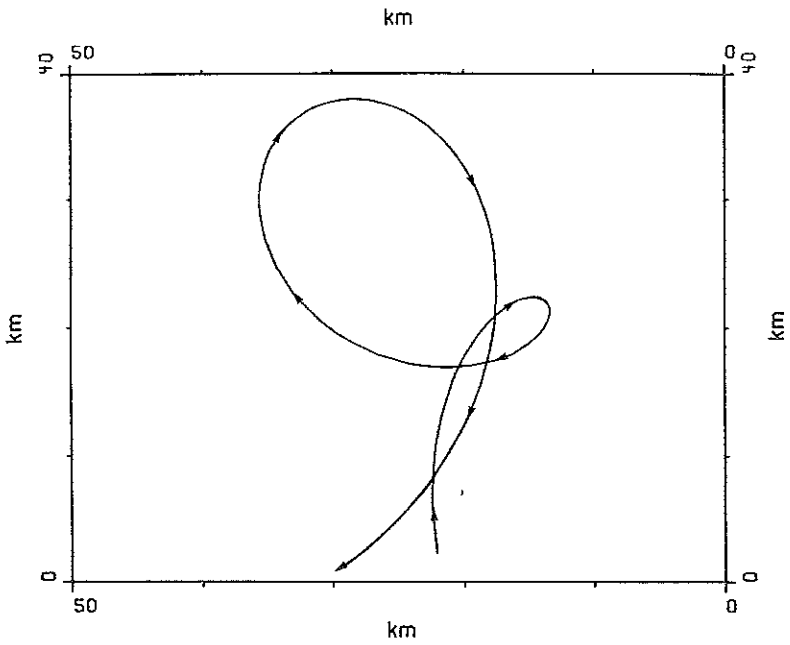

Fig. 4. A close-up of the oscillatory trajectory in the area bounded by the dashed circle in Fig. 3a.

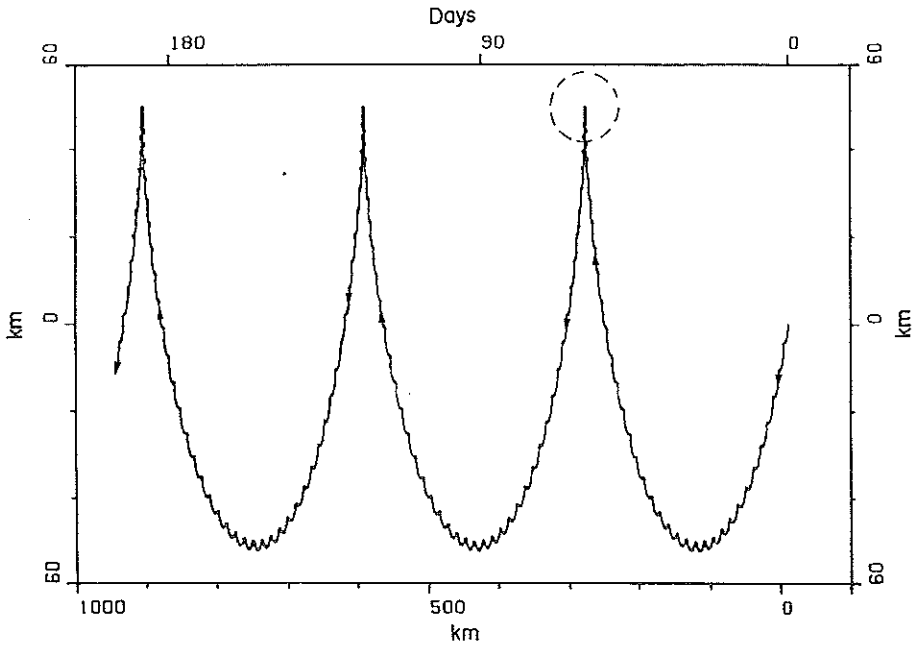

Fig. 5. The general oscillatory trajectory of a particle located at the edge of a typical deep-ocean eddy with a linear orbital velocity in mid-latitudes ($g' = 2 \times 10^{-4}$ m s^{-2}, $S = 0.0125$, $f = 0.5 \times 10^{-4}$ s^{-1}, $r_0 = 50$ km, $R_0 = 0.02$). The details of the trajectory in the area bounded by the dashed circle are shown in Fig. 6.

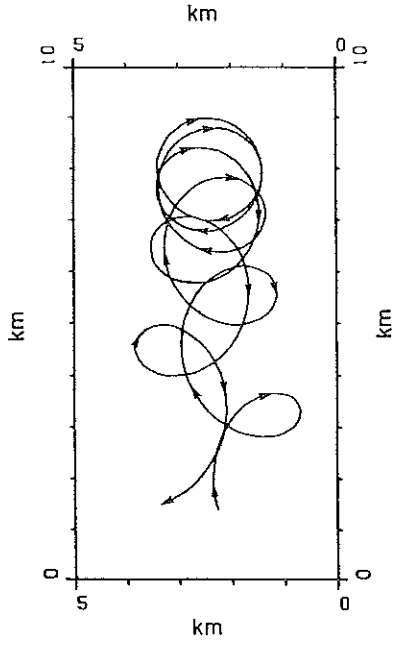

Fig. 6. A close up of the oscillatory trajectory in the area bounded by the dashed circle in Fig. 5.

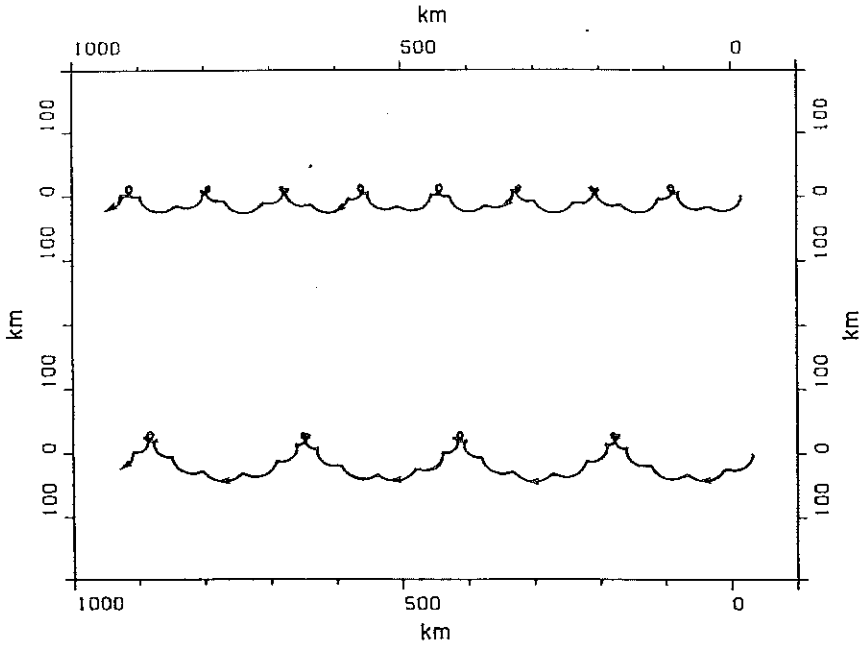

Fig. 7. The oscillatory trajectory of a particle located at a distance of $r_0/3$ (top curve) and $2r_0/3$ (lower curve) from the center of a typical low-latitude eddy with a parabolic velocity profile ($g' = 2 \times 10^{-4}$ m s^{-2}, $S = 0.01$, $f = 2 \times 10^{-5}$ s^{-1}, $r_0 = 50$ km, $R_0 = 0.2$). For this case the motion is not periodic because the ratio between the frequency of the orbital motion and the oscillatory frequency is not a rational number (see Fig. 3 for a comparison).

To illustrate the properties of an eddy with a linear orbital velocity, typical trajectories of both the time-dependent and steady migrations are shown in Figs. 3 to 6. Figures 3 and 4 show the trajectories of a particle located at the edge of a typical eddy in low latitudes and Figs 5 and 6 display the trajectories for an eddy in mid-latitudes. As already pointed out, the oscillatory migration is more pronounced in low latitudes due to the relatively small value of f and the resulting large value of $g'S/f^2$. Figures 3 to 6 show that, due to the combined effect of translation and circular motion, the trajectories are quite complicated. The particles' paths are even more complicated when the orbital velocity is not linear, as shown in Fig. 7 and in the Appendix.

Energy and stability

The existence of the additional oscillatory solution described above raises the question of whether one state is more favorable than the other. In this context, it is instructive to compare both the energy and the stability of the two classes of motion. Comparison of the energies associated with each kind of motion is of interest because physical systems tend to adopt the less energetic state if such a state exists. To perform the comparison in question, it is sufficient to consider the energies associated with the two drifts because the eddies' interiors are identical.

For the oscillatory migration, the eddy's center is initially located at $x_s = y_s = 0$ so that the energy of a unit eddy mass is

$$E_o = (C_x^2 + C_y^2)/2 + g'SY_o,$$

where $Y_o(t_s)$ is the position of the eddy center in the fixed coordinate system and the subscript o indicates that the variable in question is associated with the oscillatory drift. With the aid of (17), it is easy to show that E_o vanishes. The energy of a unit eddy mass associated with the steady drift is

$$E_c = \frac{1}{2}\left(\frac{g'S}{f}\right)^2 + g'SY_c,$$

where Y_c is the position of the isobath along which the eddy is translating and the subscript c indicates association with the constant drift $(-g'S/f)$. For $Y_c = -g'S/2f^2$, the total eddy energy vanishes showing that if the eddy is translating along this particular line then its energy is identical to that of the oscillating eddy. The energy considerations imply, therefore, that neither state is more favorable than the other, whereas the stability considerations indicate that both the oscillatory and the steady drifts are either stable or unstable.* This results from the fact that the circulations within the eddies are identical.

In view of these considerations of energy and stability, it is concluded that both migration patterns are physically relevant. The establishment of a particular migration pattern would depend on the initial conditions, i.e., the way the eddies are formed. If there is no initial migration (at $t_s = 0$), then the oscillatory migration pattern would be established subsequently. However, bottom friction would ultimately damp the oscillations causing the oscillatory pattern to asymptotically approach the steady migration case.

* GRIFFITH and LINDEN (1981) suggested that some isolated eddies with uniform potential vorticity are unstable and break up into smaller eddies, but recently KILLWORTH (1983) has shown that eddies with linear orbital speeds (i.e., nonuniform potential vorticity) are stable to small perturbations. Killworth's analysis does not prove that all deep-ocean eddies are stable but it does illustrate that at least some eddies are stable. For additional discussion of the stability question, see NOF (1983b).

Comparison to Stern's integral relation

Here we shall discuss the relationship between our main results (17 to 21a, b) and the integral constraint (for a heavy blob on a sloping bottom of a finite depth ocean) developed recently by Stern (MORY, 1983). This integrated constraint is similar to that discussed by FLIERL *et al.* (1983) and FLIERL (1984) for upper-ocean eddies on a β-plane. It involves various assumptions regarding the way that the disturbances decay away from the eddy and, for the clarity of our comparison, it is necessary to derive it from the basic equations of motion.

Consider a two-layer system with a finite upper layer as shown in Fig. 8. Note that, hereafter, variables associated with the upper and lower layer will be denoted by the subscripts 1 and 2, respectively. The depth of the upper layer is

$$h_1 = H - Sy_s - h_2 + \eta_1, \tag{24a}$$

where η_1 is the free surface displacement. The pressures can be expressed as

$$p_1 = \rho g(H + \eta_1 - z_s), \tag{24b}$$

and

$$p_2 = \rho g(H + \eta_1 - z_s) + g\Delta\rho(h_2 + Sy_s - z_s), \tag{24c}$$

so that the equations of motion for the two layers are

$$\frac{\partial u_{1s}}{\partial t_s} + u_{1s}\frac{\partial u_{1s}}{\partial x_s} + v_{1s}\frac{\partial u_{1s}}{\partial y_s} - fv_{1s} = -g\frac{\partial \eta_1}{\partial x_s}, \tag{25a}$$

$$\frac{\partial v_{1s}}{\partial t_s} + u_{1s}\frac{\partial v_{1s}}{\partial x_s} + v_{1s}\frac{\partial v_{1s}}{\partial y_s} + fu_{1s} = -g\frac{\partial \eta_1}{\partial y_s}, \tag{25b}$$

$$-\frac{\partial h_2}{\partial t_s} + \frac{\partial}{\partial x_s}(h_1 u_{1s}) + \frac{\partial}{\partial y_s}(h_1 v_{1s}) = 0, \tag{25c}$$

$$\frac{\partial u_{2s}}{\partial t_s} + u_{2s}\frac{\partial u_{2s}}{\partial x_s} + v_{2s}\frac{\partial u_{2s}}{\partial y_s} - fv_{2s} = -g\frac{\partial \eta_1}{\partial x_s} - g'\frac{\partial h_2}{\partial x_s}, \tag{26a}$$

$$\frac{\partial v_{2s}}{\partial t_s} + u_{2s}\frac{\partial v_{2s}}{\partial x_s} + v_{2s}\frac{\partial v_{2s}}{\partial y_s} + fu_{2s} = -g\frac{\partial \eta_1}{\partial y_s} - g'\left(\frac{\partial h_2}{\partial y_s} + S\right), \tag{26b}$$

$$\frac{\partial h_2}{\partial t_s} + \frac{\partial}{\partial x_s}(h_2 u_{2s}) + \frac{\partial}{\partial y_s}(h_2 v_{2s}) = 0, \tag{26c}$$

where we have taken into account that $\eta_1 \ll h_1$ and have, therefore, neglected $\partial\eta_1/\partial t_s$ in equation (25c). Equations (25c) and (26c) can be combined to

$$\frac{\partial}{\partial x_s}(h_1 u_{1s} + h_2 u_{2s}) + \frac{\partial}{\partial y_s}(h_1 v_{1s} + h_2 v_{2s}) = 0, \tag{27a}$$

so that we may define a stream function ψ_s:

$$\frac{\partial \psi_s}{\partial y_s} = -(h_1 u_{1s} + h_2 u_{2s}), \qquad \frac{\partial \psi_s}{\partial x_s} = h_1 v_{1s} + h_2 v_{2s}. \tag{27b}$$

Using Stokes' theorem, (27a) can be integrated over the whole plane giving

$$\oint_\phi (h_1 u_{1s} + h_2 u_{2s})\, dy_s - \oint_\phi (h_1 v_{1s} + h_2 v_{2s})\, dx_s = 0,$$

which, since $h_2 = 0$ outside the curve $\gamma_s(x_s, y_s, t_s) = 0$, reduces to

$$\oint_\phi h_1 (u_{1s}\, dy_s - v_{1s}\, dx_s) = 0, \tag{28}$$

where ϕ is a rectangular domain extending to infinity in all directions. Equation (28) is satisfied if either u_{1s} or v_{1s} go to zero (at infinity) faster than $1/r_s$ [where $r_s = (x_s^2 + y_s^2)^{1/2}$] or there is a closed streamline at infinity so that $(u_{1s}/v_{1u}) = (dy_s/dx_s)$.

To obtain the total balance of forces in the downhill direction ($-y_s$), equations (25b) and (26b) are multiplied by h_1 and h_2, respectively, integrated over the whole domain, and then added to form a single equation. Using (25c) and (26c), the resulting equation can be expressed as

$$\begin{aligned}
&\int_{-\infty}^{\infty}\int \frac{\partial}{\partial t_s}(h_1 v_{1s} + h_2 v_{2s})\, dx_s\, dy_s + \int_{-\infty}^{\infty}\int \frac{\partial}{\partial x_s}(h_1 u_{1s} v_{1s} + h_2 u_{2s} v_{2s})\, dx_s\, dy_s \\
&\qquad + \int_{-\infty}^{\infty}\int \frac{\partial}{\partial y_s}(h_1 v_{1s}^2 + h_2 v_{2s}^2) + f \int_{-\infty}^{\infty}\int (h_1 u_{1s} + h_2 u_{2s})\, dx_s\, dy_s \\
&= -g \int_{-\infty}^{\infty}\int (H - s y_s + \eta_1) \frac{\partial \eta_1}{\partial y_s}\, dx_s\, dy_s - \frac{g'}{2} \int_{-\infty}^{\infty}\int \frac{\partial (h_2)^2}{\partial y_s}\, dx_s\, dy_s - g' S \int_{-\infty}^{\infty}\int h_2\, dx_s\, dy_s.
\end{aligned} \tag{29}$$

Using Stokes' theorem and (28), equation (29) can be written as

$$\begin{aligned}
&\int_{-\infty}^{\infty}\int \frac{\partial}{\partial t_s}\left(\frac{\partial \psi_s}{\partial x_s}\right) dx_s\, dy_s + \oint_\phi (h_1 u_{1s} v_{1s} + h_2 u_{2s} v_{2s})\, dy_s \\
&\qquad - \oint_\phi (h_1 v_{1s}^2 + h_2 v_{2s}^2)\, dx_s + f \oint_\phi \psi_s\, dx_s \\
&= g \oint_\phi H \eta_1\, dx_s + gS \int_{-\infty}^{\infty}\int \left[\frac{\partial}{\partial y_s}(y_s \eta_1) - \eta_1\right] dx_s\, dy_s \\
&\qquad + \frac{g}{2} \oint_\phi \eta_1^2\, dx_s + \frac{g'}{2} \oint_\phi h_2^2\, dx_s - g' S \int_{-\infty}^{\infty}\int h_2\, dx_s\, dy_s,
\end{aligned} \tag{30}$$

which, by using Stokes' theorem again and taking into account that $h_2 = 0$ along some curve $\gamma_s(x_s, y_s, t_s) = 0$, reduces to

$$\oint_\phi \frac{\partial \psi_s}{\partial t_s}\,dy_s + \oint_\phi h_1 u_{1s} v_{1s}\,dy_s - \oint_\phi h_1 v_{1s}^2\,dx_s + f \oint_\phi \psi_s\,dx_s$$

$$= g \oint_\phi (H - Sy_s)\eta_1\,dx_s - gS \int_{-\infty}^{\infty}\int \eta_1\,dx_s\,dy_s + \frac{g}{2}\oint_\phi \eta_1^2\,dx - g'S \int_{-\infty}^{\infty}\int h_2\,dx_s\,dy_s. \tag{31}$$

As before, ϕ is a rectangular domain extending to infinity in both the x_s and the y_s direction.

It is further assumed that not only the blob itself is isolated but that the disturbances in the upper layer are also isolated. Specifically we assume that: (1) At infinity ψ_s goes to zero faster than $1/r_s$ so that by (27a and 28) u_{1s} and v_{1s} also go to zero faster than $1/r_s$; (2) η_1 goes to zero faster than $1/r_s^2$; and (3) $\partial\psi_s/\partial t_s$ goes to zero faster than $1/r_s$. With these assumptions all the boundary terms vanish and (31) gives the Stern's constraint

$$gS \int_{-\infty}^{\infty}\int \eta_1\,dx_s\,dy_s + g'S \int_{-\infty}^{\infty}\int h_2\,dx_s\,dy_s = 0. \tag{32}$$

By using the equations of motion in a coordinate system traveling (steadily or unsteadily) with the eddy's center and considering the assumptions mentioned above, it is possible to show that Stern's integral constraint (32) can also be written in the form

$$gS \int_R \int \eta_1\,dx\,dy + g'S \int_{\tilde{r}} \int h_2\,dx\,dy = 0, \tag{33}$$

where R is now the area bounded by a circle whose radius is infinitely large and, as before, $\tilde{r}$ corresponds to the area of the eddy (Fig. 9). Equation (33) states that the gravitational force

$$g'S \int_{\tilde{r}} \int h_2\,dx\,dy$$

is balanced by a pressure force in the upper layer. Namely, it states that the gravitational force is not only balanced by the eddy translation and acceleration as stated by (23) but also by 'lift' and drag imposed by the upper layer.

Since $h_2 = 0$ outside the eddy, the second integral in (33) can be taken over the whole plane (R) so that we have

$$\int_R \int \left(\eta_1 + \frac{\Delta\rho}{\rho} h_2\right) dx\,dy = 0. \tag{34}$$

At first sight, (34) gives the *mistaken* impression that $\eta_1 \sim 0[(\Delta\rho/\rho)h_2]$, implying that the motions in the upper layer are always of the same order as those within the eddy regardless of the upper-layer depth. This cannot be the case because it implies that a collapse of a finite length cylinder (containing heavy fluid) near the bottom of an infinitely deep ocean produces

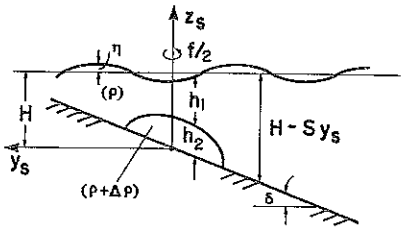

Fig. 8. Schematic diagram of the two-layer model with a finite upper layer. The free surface vertical displacement η is measured upward from the undisturbed level and $S \simeq h_2/H$.

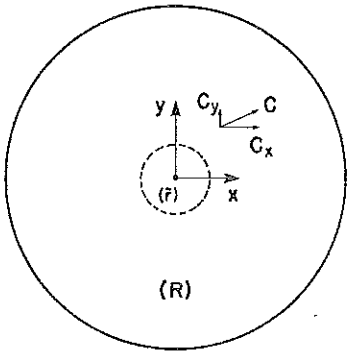

Fig. 9. Schematic diagram of the integration area in the moving coordinate system.

an infinite amount of energy which is, of course, impossible. A careful examination of (33) shows indeed that the two integrals involve two different length scales so that η_1 is not at all of the order of $(\Delta\rho/\rho)h_2$ unless $h_2 \sim 0(H)$.

To illustrate this point it is recalled that any adjustment process in the upper layer* can cause motions up to a distance of $(gH)^{1/2}/f$ away from the eddy's center. The length scale of the eddy, on the other hand, is the internal deformation radius based on the eddy's depth $(g'h_2)^{1/2}/f$. These imply that the compensating flow in the upper layer may occupy a region whose area $[\sim 0(gH/f^2)]$ is much larger than the area of the eddy $[\sim 0(g'h_2/f^2)]$. Namely, (34) implies that η_1 may be as small as

$$\eta_1 \sim 0\left[\left(\frac{\Delta\rho}{\rho}\right)^2 h_2 \left(\frac{h_2}{H}\right)\right], \tag{35}$$

and the Stern's constraint will still be satisfied. Note that according to (35) the free surface vertical displacement η_1 goes to zero as $H \to \infty$. In reality η_1 will be larger than that given by (35) because of the velocity scale.

To show this it is recalled that one can obtain a velocity scale from the potential vorticity equation for the upper layer. This scale $\{f(h_2/H)l$, where $l \sim 0[(g'h_2)^{1/2}/f]\}$ reflects the conditions that all upper-layer motions are caused by the presence of the eddy that forces the

* Such an adjustment process may be associated with either the formation of the eddy or a wake induced by the eddy's translation.

upper fluid to change its relative vorticity as it flows on top of it. Namely, the flow in the upper layer is of the order

$$u_1, v_1 \sim 0\left[(g'h_2)^{1/2}\left(\frac{h_2}{H}\right)\right], \tag{36}$$

which, upon combination with a length scale of $(g'h_2)^{1/2}/f$, gives a free surface displacement,

$$\eta_1 \sim 0[\Delta\rho/\rho h_2(h_2/H)]. \tag{37}$$

This free surface displacement is larger than that given by (35) but it also goes to zero as $H \to \infty$ supporting our assumption of a stagnant upper layer. The difference between (37) and (35) results from the fact that the disturbance (wake) in the upper layer occupies an area with the length scales $(g'h_2)^{1/2}/f$ and $(H/h_2)(g'h_2)^{1/2}/f$ both of which are smaller than the barotropic deformation radius $(gH)^{1/2}/f$.

The considerations mentioned above involve two processes. The first is associated with the generation of upper-fluid motions by the presence of the eddy ('bump') and the second is related to the region into which the induced motion spreads. In this respect the motion in the upper layer is similar to the Rossby waves radiation (from an isolated eddy) discussed by FLIERL (1984).

Finally, note that, although MORY's (1983) laboratory experiment involved upper-layer motions larger than those given by (36), there is no contradiction between the two investigations because an additional source of motion was present in Mory's experiment. It appears that, in Mory's experiment, the difference between the initial fluid level in the cylinder and the outer fluid could be directly responsible for motions as high as 10 cm s^{-1}. In other words, the presence of upper motions comparable to the eddy's internal motions was probably unrelated to relations (34) or (35) so that it does not support (or reject) any consideration.

CONCLUSIONS AND SUMMARY

Because of the limited number of available observations, it is presently impossible to tell whether or not the eddies on the deep-ocean floor (or the shelf) behave in the oscillatory manner suggested by the present model. It should be emphasized that the oscillatory migration results not only from the particular migration path but also from the properties of the migration speed. While the oscillatory path can at times be almost indistinguishable from the steady migration path [due to the smallness of the amplitude compared to the eddy size (Fig. 2b)], the oscillatory migration speed is usually very different from the steady migration speed. This results from the fact that, for deep-ocean eddies, the oscillatory speed can be of the same order as the swirl speed even if the amplitude of the oscillatory path ($g'S/f^2$) is much smaller than the eddy radius. Figure 10 shows the speeds that would be measured in mid-latitude by a fixed instrument as an eddy is passing by. Note that there is a distinct difference between the oscillatory and the steady migration.

The results of this study can be summarized as follows:

(1) An isolated lens-like eddy situated on a sloping bottom can migrate along a cycloid whose main direction is at 90° to the right of the downhill slope. As the eddy is migrating its internal structure and shape remain unaltered; namely, the time-dependent migration has no influence on the eddy's interior.

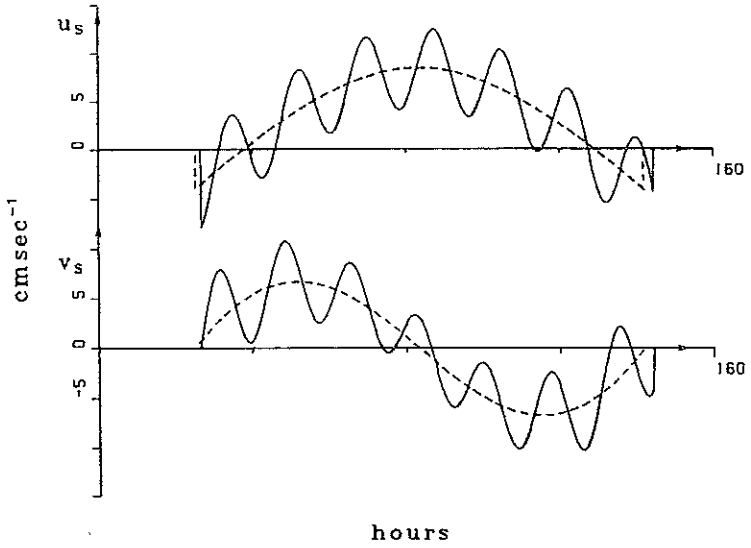

Fig. 10. The oscillatory velocities u_s and u_s (solid lines) at a fixed position ($x_s = -12$ km, $y_s = 5$ km) for a typical mid-latitude eddy with a parabolic velocity profile ($g' = 2 \times 10^{-4}$ m s^{-2}, $S = 0.02$, $f = 10^{-4}$ s^{-1}, $r_0 = 10$ km, $R_0 = 0.25$), as measured by a fixed instrument as the eddy is passing by. Steady migration velocities (dashed line) are shown for the same fixed position. Note that the regions with $u_s = v_s = 0$ on the left and right sides correspond to areas outside the eddy.

(2) The long and cross isobaths' drifts are given by

$$C_x = -\frac{g\Delta\rho S}{\rho f}(1 - \cos ft), \qquad C_y = -\frac{g\Delta\rho S}{\rho f}\sin ft,$$

where g is the gravitational acceleration, ρ and $\Delta\rho$ the density and the density difference between the blob and the environment, S the slope of the bottom, f the Coriolis parameter, and t is the time.

(3) The two main differences between the oscillatory migration and the steady drift are their migration paths and their migration speeds.

(a) *Migration paths.* The difference in the migration paths is unimportant for most mesoscale eddies in mid-latitude but is important for mesoscale eddies in low latitude. This results from the fact that the oscillatory amplitude ($g'S/f^2$) is typically ~0(1) km in mid-latitude and ~0(10) km in low latitude. Consequently, it is much smaller than the eddy size [typically 0(10) km] in mid-latitude but is comparable to the eddy size in low latitude..

(b) *Migration speed.* The difference in the migration speeds is important for both low- and mid-latitude eddies because, for deep-ocean eddies, the oscillatory speed (5 ~ 10 cm s^{-1}) can be of the same order as the swirl speed (even if the oscillatory amplitude is much smaller than the eddy size).

These results demonstrate that cold eddies on a sloping bottom can have two distinctly different migration patterns. Both cases are physically relevant and no case is more favorable than the other. If the initial conditions associated with the blob's formation are such that the blob has no translation, then the oscillatory migration would be established. However, bottom friction would probably damp the oscillations causing the migration pattern to asymptotically approach the steady drift.

APPENDIX

Solution for an eddy with a parabolic orbital speed

For this eddy [i.e., $v_\theta = 2R_0 fr[(r/r_0) - 1]$, where r is the eddy radius] the complete solution is found to be

$$u_s = 2R_0 f\left[y_s + \frac{g'S}{f^2}(1-\cos ft_s)\right] \times \left\{1 - \left[\left[x_s + \frac{g'S}{f}\left(t_s - \frac{1}{f}\sin ft_s\right)\right]^2 + \left[y_s + \frac{g'S}{f^2}(1-\cos ft_s)\right]^2\right]^{1/2}\Big/ r_0\right\} - \frac{g'S}{f}(1-\cos ft_s), \quad \text{(A1)}$$

$$v_s = -2R_0 f\left[x_s + \frac{g'S}{f}\left(t_s - \frac{1}{f}\sin ft_s\right)\right] \times \left\{1 - \left[\left[x_s + \frac{g'S}{f}\left(t_s - \frac{1}{f}\sin ft_s\right)\right]^2 + \left[y_s + \frac{g'S}{f^2}(1-\cos ft_s)\right]^2\right]^{1/2}\Big/ r_0\right\} - \frac{g'S}{f}\sin ft_s, \quad \text{(A2)}$$

$$h_s = \hat{h} + R_0 f^2(2R_0 - 1)\left\{\left[x_s - \frac{g'S}{f}\left(t_s - \frac{1}{f}\sin ft_s\right)\right]^2 + \left[y_s + \frac{g'S}{f^2}(1-\cos ft_s\right]^2\right\}\Big/ g' + 2R_0(1-4R_0)f^2\left\{\left[x_s + \frac{g'S}{f}\left(t_s - \frac{1}{f}\sin ft_s\right)\right]^2 + \left[y_s + \frac{g'S}{f^2}(1-\cos ft_s)^2\right]^2\right\}^{3/2}\Big/ 3g'r + R_0^2 f^2\left\{\left[x_s + \frac{g'S}{f}\left(t_s - \frac{1}{f}\sin ft_s\right)\right]^2 + \left[y_s + \frac{g'S}{f^2}(1-\cos ft_s)\right]^2\right\}^2\Big/ g'r_0^2. \quad \text{(A3)}$$

The corresponding trajectories are found, as previously, by replacing u_s and v_s by dx_s/dt_s and

dy_s/dt_s and solving the resulting equations. One finds

$$X_s(t_s) = r_i \cos\left[-2R_0 f(1 - r_i/r_0)t_s + \theta_i\right] - \frac{g'S}{f^2}(ft_s - \sin ft_s), \tag{A4}$$

$$Y_s(t_s) = r_i \sin\left[-2R_0 f(1 - r_i/r_0)t_s + \theta_i\right] - \frac{g'S}{f^2}(1 - \cos ft_s), \tag{A5}$$

where, as before, r_i and θ_i are the particle's initial radius and angle. (The migration path is shown in Fig. 7.)

Acknowledgements—Computations and plots were made by S. VanGorder. I thank P. Killworth for useful comments and G. Flierl for helpful discussions. The study was supported by the Office of Naval Research Contract No. N00014-82-C-0404 and by the Florida State University. .

REFERENCES

ARMI L. and E. D'ASARO (1980) Flow structures of the benthic ocean. *Journal of Geophysical Research*, **85**, 469–484.

CSANADY G. T. (1979) The birth and death of a warm core ring. *Journal of Geophysical Research*, **84**, 777–780.

FLIERL G. R. (1979) A simple model for the structure of warm and cold core rings. *Journal of Geophysical Research*, **84**, 781–785.

FLIERL G. R. (1984) Rossby wave radiation from a strongly nonlinear warm eddy. *Journal of Physical Oceanography*, **14**, 47–58.

FLIERL G., M. E. STERN and J. WHITEHEAD (1983) The physical importance of modons: laboratory experiments and integral constraints. *Dynamics of Atmospheres and Oceans*, **7**, 233–263.

GRIFFITH R. W. and P. F. LINDEN (1981) The stability of vortices in a rotating, stratified fluid. *Journal of Fluid Mechanics*, **105**, 283–316.

HOUGHTON R. W., R. SCHLITZ, R. C. BEARDSLEY, B. BUTMAN and J. C. CHAMBERLIN (1982) The Middle Atlantic Bight cold pool: evolution of the temperature structure during summer 1979. *Journal of Physical Oceanography*, **12**, 1019–1029.

KILLWORTH P. D. (1983) On the motion of isolated lenses on a beta-plane. *Journal of Physical Oceanography*, **13**, 368–376.

MCDOWELL S. E. and H. T. ROSSBY (1978) Mediterranean water: an intense mesoscale eddy off the Bahamas. *Science, Wash.*, **202**, 1085–1087.

MORY M. (1983) Theory and experiment of isolated baroclinic vortices. Technical Report, Woods Hole Oceanographic Institute, WHOI-83-41, pp. 114–132.

NOF D. (1981) On the β-induced movement of isolated baroclinic eddies. *Journal of Physical Oceanography*, **11**, 1662–1672.

NOF D. (1982) On the movement of deep mesoscale eddies in the North Atlantic. *Journal of Marine Research*, **40**, 57–74.

NOF D. (1983a) The translation of isolated cold eddies on a sloping bottom. *Deep-Sea Research*, **30**, 171–182.

NOF D. (1983b) On the migration of isolated eddies with application to Gulf Stream rins. *Journal of Marine Research*, **41**, 399–425.

OU H. W. and R. HOUGHTON (1982) A model of the summer progression of the cold-pool temperature in the Middle Atlantic Bight. *Journal of Physical Oceanography*, **12**, 1030–1036.